Coronin 3 involvement in F-actin-dependent processes at the cell cortex

Elsevier Editorial System(tm) for Experimental Cell Research

Manuscript Draft

Manuscript Number:

Title: Coronin 3 involvement in F-actin dependent processes at the cell cortex

Article Type: Research Article

Section/Category:

Keywords: Coro1C; CRNN4; WD40-repeat; F-actin; cell motility; cytoskeleton; siRNA

Corresponding Author: Dr. Christoph Stephan Clemen,

Corresponding Author's Institution: Institute of Biochemistry I

First Author: André Rosentreter

Order of Authors: André Rosentreter; Andreas Hofmann; Charles-Peter Xavier; Maria Stumpf; Angelika Anna Noegel; Christoph Stephan Clemen

Manuscript Region of Origin:

Abstract: The actin interaction of coronin 3 has been mainly documented by in vitro experiments. Here, we discuss coronin 3 properties in the light of new structural information and focus on assays that reflect in vivo roles of coronin 3 and its impact on F-actin associated functions. Using GFP-tagged coronin 3 fusion proteins and RNAi silencing we show that coronin 3 has roles in wound healing, protrusion formation, cell proliferation, cytokinesis, endocytosis, axonal growth, and secretion. During formation of cell protrusions actin accumulation precedes the focal enrichment of coronin 3 suggesting a role for coronin 3 in events that follow the initial F-actin assembly. Moreover, we show that coronin 3 similar to other coronins interacts with the Arp2/3-complex and cofilin indicating that this family in general is involved in regulating Arp2/3 mediated events.

INSTITUT FÜR BIOCHEMIE I

Medizinische Fakultät
Universität zu Köln

Dr. Christoph S. Clemen
Joseph-Stelzmann-Str. 52
50931 Köln
Tel.: +49 221 478-6980
Fax: +49 221 478-6979
E-Mail:christoph.clemen@uni-koeln.de

EXPERIMENTAL CELL RESEARCH

Cologne, 16.10.2006

Manuscript submission

Dear Editor,

please find enclosed our manuscript entitled "Coronin 3 involvement in F-actin dependent processes at the cell cortex" for publication in *Experimental Cell Research*.
In this manuscript we present for the first time a detailed analysis of the biological function of the WD40-repeat protein coronin 3. Our experiments suggest an important role for coronin 3 in F-actin dependent cellular processes.

Sincerely yours,

Christoph S. Clemen

Coronin 3 involvement in F-actin dependent processes at the cell cortex

André Rosentreter[a], Andreas Hofmann[b], Charles-Peter Xavier[a], Maria Stumpf[a], Angelika A. Noegel[a,c], Christoph S. Clemen[1,#]

[a]Center for Biochemistry, Institute of Biochemistry I, Medical Faculty, and [c]Center for Molecular Medicine, University of Cologne, Joseph-Stelzmann-Str. 52, 50931 Cologne, Germany; [b]Institute of Structural & Molecular Biology, School of Biological Sciences, The University of Edinburgh, Michael Swann Building, The King's Buildings, Mayfield Road, Edinburgh EH9 3JR, Scotland

[#]Author for correspondence:

C. S. Clemen, Institute of Biochemistry I, Medical Faculty, University of Cologne, Joseph-Stelzmann-Str. 52, 50931 Cologne, Germany

Phone: +49-221-478-6980

Fax: +49-221-478-6979

E-Mail: christoph.clemen@uni-koeln.de

Abstract

The actin interaction of coronin 3 has been mainly documented by *in vitro* experiments. Here, we discuss coronin 3 properties in the light of new structural information and focus on assays that reflect *in vivo* roles of coronin 3 and its impact on F-actin associated functions. Using GFP-tagged coronin 3 fusion proteins and RNAi silencing we show that coronin 3 has roles in wound healing, protrusion formation, cell proliferation, cytokinesis, endocytosis, axonal growth, and secretion. During formation of cell protrusions actin accumulation precedes the focal enrichment of coronin 3 suggesting a role for coronin 3 in events that follow the initial F-actin assembly. Moreover, we show that coronin 3 similar to other coronins interacts with the Arp2/3-complex and cofilin indicating that this family in general is involved in regulating Arp2/3 mediated events.

Keywords

Coro1C, CRNN4, WD40-repeat, F-actin, cell motility, cytoskeleton, siRNA

Introduction

Coronin 3 (coronin 1C, CRNN4) is a member of the coronin protein family, which consists of seven proteins in mammals. Coronins represent one of the many subfamilies of the WD40-repeat-domain proteins, which were discovered by Fong et al. [1] and are defined by the presence of at least four WD40-repeats in the core of the protein. Recently, the crystal structure of a truncated coronin 1 protein has been solved and revealed the presence of seven WD40-repeat domains [2]. The repeats are thought to serve as a stable platform for protein-protein interactions. Several WD-repeat proteins have been linked to human diseases [3,4].

Coronins are highly conserved but poorly understood proteins. They play a central role in various cellular processes including signal transduction, transcriptional regulation, remodelling of the cytoskeleton, and regulation of vesicular trafficking. The coronin protein family can be divided into two distinct subfamilies, short coronins and long coronins [5]. Coronin 3 is a member of the short coronin subfamily. In human and mouse it consists of 474 amino acids with a sequence-derived molecular weight of 53 kDa, the apparent molecular weight by SDS-PAGE analysis is 57 kDa. Coronin 3 is expressed in all tissues and was described as an F-actin bundling and crosslinking protein. Coronin 3 localizes to the leading edges of a cell, to pseudopodia, and the submembranous cytoskeleton [6,7].

F-actin association has been reported for most coronin proteins. The actin cytoskeleton plays crucial roles in cell locomotion, cytokinesis, cell-to-cell interaction, and establishment and maintenance of cellular morphology. The diversity of F-actin structures and associated cellular functions depends on many actin-binding proteins [8,9]. The submembranous area of a cell is enriched in branched F-actin filaments and the Arp2/3 complex [10,11]. Prime examples of a cellular function involving branched F-actin are the formation of lamellipodia and cellular motility. The Arp2/3

complex is enriched in the periphery of lamellipodia and plays a key role in forming a short-branched F-actin network that generates the protruding force depending on a locally well-organized assembly and disassembly of F-actin [12,13]. The Arp2/3 complex consists of seven subunits. p34 (Arc35, ARPC2) together with ARPC4 forms the center of the Arp2/3 complex which initiates site-directed branching and elongation of actin filaments and nucleates new actin filaments [14-17]. Surprisingly Arp2/3 inhibition by siRNA konckdown in neurite growth cones was found to minimally affect actin organization [18] pointing out that branched filaments are also generated by other mechanisms such as crosslinking by filamins [19].

For the yeast coronin an inhibitory action on the actin nucleation activity of the Arp2/3 complex was recently reported which was most likely achieved through interaction with its Arc35 subunit [20,21]. Likewise, mammalian coronin 2 was shown to bind to the p34 subunit of the Arp2/3 complex [22], however the interaction site on the coronin molecule has not been identified. The F-actin binding and bundling activity of coronin 3 occurs C-terminally (aa 315-444) to the coiled coil domain (aa 444-474), which mediates trimerization [6,23]. Moreover, the entire C-terminus of coronin 3 recruits the N-terminus to F-actin filaments [6]. Additionally, we previously have identified a highly basic 12 amino acid motif in the N-termini of all short coronins (rvvrqskfrhvf; pI = 12.3; [5]) and this region has been proposed to be involved in the actin interaction [24].

Here, we elucidate the structure of coronin 3 based on the recent X-ray data of coronin 1 and investigate the role of coronin 3 in cellular processes that involve the activity of the actin cytoskeleton by employing overexpression of coronin domains, by down-regulating the coronin 3 levels using the RNAi technique, and by co-immunoprecipitation.

Materials and Methods

CD-spectroscopy and thermal denaturation

CD spectra of peptide samples (1.8 µM) were recorded in 20 mM NaCl, 5 mM HEPES, pH 7.5, at 20°C using a Jasco J-810 spectropolarimeter equipped with a Peltier element. All spectra were corrected against the baseline and the data were transformed into mean residue ellipticity using the programme ACDP [25]. For thermal denaturation experiments, the CD signal at 222 nm was monitored from 20°C to 80°C with a heating rate of 1 K/min. Data were recorded at 0.5 K increments. Unfolding experiments were performed three times independently. Changes in the mean residue ellipticity at 222 nm were used to construct an unfolding curve. Curve fitting was done with SigmaPlot using a sigmoidal equation.

Generation of EGFP-fusion constructs of coronin 3 domains

Plasmids EGFP-Coro3NWDC (human, full length, aa 1-474, NM_014325), EGFP-Coro3ΔCC (aa 1-444), and EGFP-Coro3ΔNC (aa 72-404) are described in Spoerl et al. [6]. pEGFP-Coro3WD (aa 72-299), pEGFP-Coro3NC (aa 1-71 fused to aa 300-474), and pEGFP-Coro3NGC (aa 1-71 fused to aa 300-474 via a 5-glycine loop), which code for truncated EGFP-coronin 3 fusion proteins were cloned into pEGFP-C1 (Clontech). The respective fragments were generated by PCR using pEGFP-Coro3NWDC as template. For pEGFP-Coro3WD the fragment WD was amplified using the primers CCCAAGCTTCTTCTTACCCTACAGTATGTGGC and CGCGGATCCGGATTCATCCGTGATCTCAAAATAG. To create pEGFP-Coro3NC and pEGFP-Coro3NGC the N-terminal fragment encoding amino acids 1-71 (fragment N) was amplified using the primers CCCAAGCTTCTATGAGGCGAGTGGTACGACAGAGC and GCCGGTACCTTTGTCAATTCGACCAGTCTTGTGC, the C-terminal fragment

encoding amino acids 300-474 (fragment C) was amplified by primer pair CGGGGTACCCCGTACGTCCACTACCTCAACACATTC and CGCGGATCCTCAGGCTGCTATCTTTGCCATCTG, and fragment GC containing a glycine loop (5 glycine residues) between the N- and C-terminus was amplified using CCGGGTACCGGAGGAGGAGGAGGACCGTACGTCCACTACCTCAACACA and CGCGGATCCTCAGGCTGCTATCTTTGCCATCTG primers. The PCR-products were cloned into pGEM-T Easy vector (Promega) and verified by sequencing. For plasmids EGFP-Coro3NC and EGFP-Coro3NGC fragment N was inserted as HindIII/KpnI fragment into pEGFP-C1, followed by addition of the C and GC KpnI/BamHI fragments, respectively. The insert WD was cloned as HindIII/BamHI fragment into pEGFP-C1. Plasmid DNA used for transfection was prepared and purified using Nucleobond AX plasmid midi kits (Macherey & Nagel). The term Coro3WT refers to the endogenous coronin 3 protein.

The retroviral vector GFP-hCoro3-BMN was generated by blunt end cloning of an AgeI/BamHI-GFP-hCoro3 cassette retrieved from EGFP-Coro3NWDC into the BamHI/NotI-backbone of pBMN-Z (Shigemi Kinoshita, Nolan Lab, Stanford University; http://www.stanford.edu/group/nolan/plasmid_maps/pmaps.html).

A plasmid coding for RFP-actin was kindly provided by Stefan Wöll (University of Mainz).

Subcellular fractionation and immunoblotting

For western blot analysis mammalian cells were lysed in RIPA buffer (150 mM NaCl, 50 mM Tris-HCl, pH 8.0, 0.1% sodium dodecyl sulfate, 1% Nonidet P-40, 0.5% deoxycholic acid) supplemented by phenylmethylsulfonyl fluoride (PMSF, 0.1 mM) and complete protease inhibitor mixture (Roche). After pelleting of the cell debris, RIPA-supernatants or the fractions of the differential centrifugation were subjected to

standard SDS-PAGE (12% acrylamide) and proteins were blotted onto Protran nitrocellulose membranes (Schleicher and Schüll) according to Laemmli [26] and Towbin et al. [27]. Detection of coronin 3 was done with mAb K6-444 [5], ß-actin was detected by mAb AC 40 (Sigma) followed by incubation with goat anti-mouse IgG coupled to horseradish peroxidase (Sigma) and enhanced chemiluminescence.

Differential centrifugation was done according to Spoerl et al. [6]. For F-actin depolymerization, confluent HaCaT or HEK293 cell monolayers were incubated in normal cell culture medium containing 5 µM latrunculin B (30 min; Sigma). Cells were then washed with PBS with or without 0.2% Triton X-100 as indicated, followed by two additional washes with PBS, and lysed in HES buffer (20 mM Hepes, pH 7.2, 1 mM EDTA, 0.25 M sucrose) containing complete protease inhibitor mixture (Roche). Cells were disrupted with 15 strokes of a tight fitting Dounce homogenizer and nuclei and unbroken cells were removed by centrifugation at 500xg for 10 min. Supernatants were further fractionated by centrifugation at 2,000xg (10 min), 10,000xg (30 min), and 100,000xg (60 min). All pellet fractions were resuspended in HES buffer, re-centrifuged, and finally resuspended in a volume according to the respective supernatant. Sample volumes of the PBS/Triton X-100 washing steps and the centrifugation steps were normalized to the original number of cells used.

Mammalian cell culture, transfection, generation of stably transfected cell lines, and retroviral transduction

HEK293 human embryonic kidney cells (ATCC: CRL-1573) and HaCaT human keratinocytes [28] were grown in Dulbecco's modified Eagle's Medium (DMEM, 4.5 g/l glucose, Sigma) supplemented with 10% fetal calf serum (Biochrom), 1 mM sodium pyruvate (Sigma), 2 mM L-glutamine (Sigma), 100 units/ml penicillin G, and 100 µg/ml streptomycin (Invitrogen). In case of NIH3T3 murine fibroblasts (ATCC:

CRL-1658) DMEM with 1 g/l glucose was used. PC-12 cells (ATCC: CRL-1721) were cultured in suspension in RPMI 1640 medium with 25 mM Hepes pH 7.4, supplemented with 10% horse serum, 5% FCS, 4 mM L-glutamine, 100 U/ml penicillin G and 100 µg/ml streptomycin. All cells were grown at 37°C with 5% CO_2.

To induce differentiation, PC-12 cells were seeded on poly-L-lysine (MW > 300,000; Sigma) coated culture dishes up to 40% confluency and differentiation was induced by supplementing with nerve growth factor 7S (NGF; Invitrogen, 13290-010) in a final concentration of 50 ng/ml.

Transfection of HEK293 cells and PC-12 cells was done by electroporation (200 V, 975 µF). Stably transfected HEK293 cell clones were selected in culture medium containing 1,200 µg/ml geneticin (G418; Invitrogen). Transient transfection of PC-12 cells was performed 24 h before inducing differentiation and the expression of the fusion proteins persisted for seven days.

To stably express Coro3NWDC in HaCat cells they were retrovirally transduced according to [29]. For production of retroviruses, ΦNX-E cells were seeded at 2 x 10^6 cells on 60 mm dishes and transfected the next day with the retroviral vector GFP-hCoro3-BMN using Lipofectamine (Invitrogen). Retroviral supernatant was collected 24h, 48h and 72h after transfection and used for infection of the target HaCat cells according to [30] and www.stanford.edu/group/nolan/protocols/pro_helper_free.html.

RNAi silencing

To reduce the amount of coronin 3 protein a siRNA SMARTpool directed against murine coronin 3 was obtained from Dharmacon (CORO1C, Cat # M-007778-00-50), which had been derived from sequence NM_011779. The siRNA pool contains four different siRNA complexes. On day 1 murine NIH3T3 fibroblasts were trypsinized, counted, and seeded into a 24-well-plate to reach a confluency of 40% for

transfection. The culture medium was free of antibiotics. On day 2 and 3 cells were transfected with 100 nM siRNA using oligofectamine (Invitrogen) according to the included protocols. Wound healing assays, immunofluorescence, and western blotting were done 72 h after the first siRNA transfection. To visualize the transfection efficiency cells were transfected with a Cy3-tagged siRNA directed against luciferase GL2. Control cells were treated with oligofectamine or the luciferase siRNA only. Due to the experimental design, this transient transfection of RNAi duplexes cannot be used for the other assays described.

Immunofluorescence, confocal microscopy, and life cell imaging

To visualize endogenous coronin 3 and F-actin, HaCaT cells were either first fixed in 4°C cold 4% paraformaldehyde for 20 min followed by permeabilization with 0.5% Triton X-100 in PBS or first permeabilized and then fixed. HEK293 cells were fixed and then permeabilized. Immunostaining was performed according to Spoerl et al. [6]. Secondary IgG were goat anti-mouse coupled to Alexa 488 or Cy3 (Molecular Probes and Sigma). F-actin was labelled by incubation for 60 min with 200 ng/ml TRITC- or FITC-phalloidin (Sigma), nuclei were visualized by incubation for 60 min with 100 ng/ml DAPI (Sigma), both together with the secondary antibody. Appropriate control experiments were performed. Images were recorded with a Leica DM IRBE microscope and TCS SP confocal laser scanning technology with TCSNT software. Image processing was done with Adobe Photoshop.

For cell migration and cell activity assays live cell imaging was performed using the Leica DM IRE 2 microscope and Leica DFC 350 FX camera with Leica FW 4000 software. In all these experiments cells were grown at 37°C with 5% CO_2.

In vitro wound healing, proliferation, cytokinesis, and cell activity assay

For *in vitro* wound healing a confluent layer of stably transfected HEK293 cells or of siRNA treated NIH3T3 cells was scratched with a 27-gauge needle. The culture medium was changed to remove detached cells or debris. Closure of the wound was followed by recording an image every ten minutes with the equipment described above. For calculation of the velocity of the wound healing the distance of the wound borders at 1 h and 11 hrs after scratching were determined in at least three positions. Three (HEK293) or four (NIH3T3) independent experiments were performed.

To measure the proliferation rate, stably transfected HEK293 cells were seeded at 10^6 cells per 10 cm culture dish. After three days the cells from three independent experiments were trypsinized and counted again.

To reveal defects in the cytokinesis, stably transfected HEK293 cells were seeded at 10^5 cells per 10 cm culture dish and the relative amounts of multinuclear cells were determined by fluorescent microscopy after three days of cultivation from two independent experiments.

To visualize the activity of stably transfected HEK293 cells, they were seeded at low concentrations. 12 hours later the GFP fluorescence signal of single cells was recorded for 30 minutes with a Leica DM IRE 2 microscope and a Leica DFC 350 FX camera with Leica FW 4000 software. For each population the number of forming and retracting protrusions of single cells were determined. Similarly, the dynamics of GFP-coronin 3 and RFP-actin were recorded by confocal microscopy (Leica DM IRBE microscope and TCS SP confocal laser scanning technology) in double-transfected HEK293 cells. Every 10 seconds a 3-fold averaged image of single cellular protrusions was taken.

Receptor-mediated transferrin endocytosis and HRP fluid phase pinocytosis

To measure the receptor mediated endocytosis of transferrin, 10^5 HEK293 cells seeded on coverslips were incubated for five hours in serum-reduced (0.1% FCS) culture medium at 37°C. After two washes with PBS, the cells were incubated for 30 minutes at 37°C in serum-free medium containing 5 µg/ml transferrin/Texas Red (Molecular Probes). Confocal images were recorded as described above. Identical recording parameters were used throughout the individual experiments. Using Adobe Photoshop, forty single cells from two independent experiments of each cell population were framed, a histogram of the signal intensity of the enclosed area was calculated, and the mean values of the Texas Red signal intensities were used for statistical analysis.

Uptake of the fluid phase marker horseradish peroxidase (HRP) was determined in stably transfected HEK293 cell lines. Cells (80% confluence) were washed with PBS (Ca^{2+} and Mg^{2+} free) and then incubated at 37°C with HRP (2 mg/ml) in DMEM, containing 0.1% bovine serum albumin and 10 mM HEPES, pH 7.4, for 60 min. Dishes were placed on ice, washed four times with ice-cold DMEM, supplemented with 10 mM HEPES, pH 7.4, and five times with PBS. Cells were scraped off at 4°C with PBS, containing 1% Triton X-100. After centrifugation at 10,000 g for 10 min at 4°C, aliquots of the supernatants were processed by the 1-Step Turbo TMB enzyme-linked immunosorbent assay kit (Pierce Chemical). HRP activity was determined at 450 nm (Labsystems Multiscan RC) after 20 minutes of incubation with the substrate 3,3',5,5'-tetramethylbenzidine at 37°C and addition of 1M sulfuric acid. The activity was normalized to the total protein concentration. The experiment was done three times with three determinations of every sample.

Norepinephrine secretion and neurite outgrowth of PC-12 cells

PC-12 cells transiently transfected with EGFP-coronin 3 expression constructs were seeded in equal amounts of 10^6 cells per 60 cm poly-L-lysine coated culture dish. The different cell populations were further cultured in the absence or presence of NGF at a final concentration of 50 ng/ml. Every other day 3 ml of the culture medium were collected and the norepinephrine (noradrenaline) concentration was measured in duplicate in samples of 300 µl using the norepinephrine EIA (Labor Diagnostika Nord). At the end of the experiment the cells were trypsinized and counted again to standardize the norepinephrine concentration values. The experiment was carried out twice. The neurite length of about 50 transfected cells of each population from two independent experiments were assayed after four days of NGF treatment. Neurite (axon) lengths of PC-12 cells were defined as the distances from the tip of a neurite to the junction between neurite base and the cell body and are given relative to the respective cell somata.

Co-immunoprecipitation

$1.5x10^8$ HEK293 cells (non-confluent culture dishes) stably transfected with EGFP-Coro3NWDC were treated for 30 min with 5 µM latrunculin B (Sigma) in order to prevent unspecific co-precipitation of proteins bound to F-actin, washed twice with PBS, resuspended in 6 ml immunoprecipitation (IP) buffer (0.33 x PBS pH 7.4, 2 mM benzamidine, 4 mM DTT, 2 mM EDTA, 0.5 mM PMSF, 0.5% Triton X-100 (added after sonication)), sonicated, and microscopically examined to confirm complete cell lysis. The resulting lysate was centrifuged at 2,000xg for 3 min at 4°C and precleared prior to immunoprecipitation with equilibrated Protein G sepharose beads for 30 min. 3 ml of pre-cleared supernatant were incubated with 500 µl of anti-GFP mAb (K3-184 or K3-167; $(NH_4)_2SO_4$-concentrated hybridoma supernatant; [31]), 7 µl Triton X-100

and 70 µl protein G sepharose beads at 4°C for 1.5 hrs. The beads were washed four times with 1 ml IP buffer, incubated with 2x SDS-sample buffer for 5 min at 95°C, and analyzed by immunoblotting using antibodies specifically recognizing coronin 3, p34-Arc (rabbit polyclonal Ab, Upstate), and cofilin (rabbit polyclonal Ab, Sigma). For control, the experiment was carried out with cell lysate or with anti-GFP-mAb only. Immunoblotting with anti-BiP/GRP78 (Transduction Laboratories) and anti-ß-actin (Sigma) was used for control to test for the specificity of immunoprecipitation. The experiment was done several times.

Statistical analysis

Statistical analysis was performed using ANOVA or Student's t-test, as appropriate. The exact probability values and the significance of an analysis as well as the number of independent experiments and repeated measurements are indicated.

Results

Interaction of coronin 3 with the F-actin cytoskeleton in vivo

In HaCaT cells endogenous coronin 3 localizes to the submembranous actin cytoskeleton. This localization is particularly obvious in cells, which exhibit a strong accumulation of actin filaments underneath the plasma membrane. Coronin 3 additionally was detected at punctate structures in the cytoplasm, with a perinuclear accumulation of these spots (Fig. 1A, first panel). An identical pattern was observed when HaCat cells were retrovirally transduced to express GFP-coronin 3 (Fig. 1A, first panel, inset, for comparison given in red). The cortical localization of endogenous coronin 3 is maintained after Triton X-100 permeabilization prior to fixation (Fig. 1A, third panel and insets), indicating a stable association of coronin 3 and F-actin *in*

vivo. By contrast, HaCaT cells treated with latrunculin B prior to fixation do not show such a coronin 3 distribution. Coronin 3 accumulates in spots clearly distinguishable from the remaining F-actin staining (Fig. 1A, second panel). The latter F-actin structures represent a pool that is resistant to the treatment with latrunculin B [32]. HaCaT cells treated with latrunculin B and Triton X-100 prior to fixation did neither show a structured staining of coronin 3 nor of F-actin (Fig. 1A, fourth panel); most of both proteins was gone and only a diffuse residual staining remained. These observations were confirmed by differential centrifugation and immunoblotting (Fig. 1B). The relative distribution within the different fractions of each experiment can be compared. In untreated HaCaT cells coronin 3 is most abundant in the 100,000 g pellet, minor amounts are detectable in the 10,000 g pellet and in the 100,000 g supernatant. The 10,000 g pellet contains the crude cytoskeletal fraction, the pellet of 100,000 g includes membranes with cytoskeletal elements, and the supernatant of 100,000 g contains the cytosolic fraction. The majority of coronin 3 is detected in the Triton X-100 wash of the cells prior to the harvest. After treatment with latrunculin B the amount of coronin 3 in the 100,000 g pellet is markedly reduced and instead appears in the 100,000 g supernatant. This immunofluorescence and differential centrifugation data and the results of our previous study [6] clearly demonstrate a localization of coronin 3 that depended strongly on F-actin *in vitro* as well as *in vivo*.

Implications from the coronin 1 crystal structure for coronin 3 and individual domains

Up to now coronin 3 like all short coronin proteins was thought to consist of a N-terminal domain (aa 1-71), a core region containing five WD40-domains (aa 72-299), and a C-terminal domain (aa 300-474) [5,33]. A crystal structure of N- and C-terminally truncated coronin 1 (aa 10 - aa 400) has been resolved and revealed the

presence of seven WD40-repeat domains [2]. Based on these data, coronin 3 may contain two additional WD40-repeats as well that are atypical in sequence and in their structure and are located in the regions referred to as N-terminus (aa 1-71) and conserved part of the C-terminus (aa 300-404) (Fig. 2A). Amino acids 1-11 as well as 348-404 do not contribute to the respective WD40-repeats.

The structure of coronin 1 was determined at 1.75 Å and allowed a description of the overall shape of the protein as well as intramolecular interactions [2]. In addition to the overall structure similar intramolecular interactions may occur which stabilize the coronin 3 structure. Therefore, Tyr362 of coronin 3 may interact with Val327/Glu331 and with a loop containing Arg352, Ser354, Leu356, Gln358, and Asp360 that arches between the 7th propeller and Tyr362. These interactions most likely maintain the structural stability of the C-terminal domain of coronin 3. In addition Lys9 of the N-terminus can interact with Asp360 of this C-terminal loop. According to the crystal structure of coronin 1 several more interactions of the N-terminal 71 aa of coronin 3 with the C-terminal aa 300-474 occur and can stabilize the overall tertiary structure [2].

Analyses of structure and electrostatic potential of the surface of coronin 1 resulted in the identification of potential F-actin binding sites comprising a region on the top of propellers 1, 6, 7, and a second region on the bottom side of propellers 6 and 7 including parts of the C-terminal extension [2]. These properties as well can be assigned to coronin 3. Fragments of coronin 3 exactly comprising these interacting regions were used in our previous *in vitro* binding studies [6]. The binding characteristics of the N-terminal and C-terminal peptides among each other and F-actin are in good agreement with the structural results obtained from coronin 1.

We now additionally employed CD spectroscopy and thermal denaturation assays to address the question if the coronin 3 fragments comprising aa 300-474 and aa 315-

444 (lacking the very C-terminal coiled coil) containing single WD40-domains fold properly. The secondary structure estimation from CD spectra correlated with the sequence derived prediction (Fig. 2A). In a second step the folding stability was determined by heating the samples at a rate of 1 K/min and monitoring the CD-signals (Fig. 2B). Both peptides showed a standard two-state unfolding behaviour, but with a higher transition temperature for the full-length C-terminus (T1/2=47°C) compared to the shorter polypeptide (T1/2=42°C) which points to intramolecular interactions of the extra C-terminal region.

We conclude that coronin 3 fragments that do not include all seven WD40-repeats still fold properly and form functional domains that retain the F-actin binding activity they have in the full-length coronin 3 protein.

Subcellular localization of endogenous coronin 3 and coronin 3 domains fused to EGFP

Previously we showed that truncated coronin 3 (aa72-404, Coro3ΔNC), which lacks the N-terminus (aa 1-71) and the unique C-terminal region (aa 405-474), alters the outgrowth of neuronal axons in PC-12 and neuro-2a cells [7]. Expression of Coro3ΔNC in HEK293 cells changed the cell morphology to a spindle like form. Coro3ΔCC lacking the coiled coil domain (444-474) was diffusely distributed throughout the cell and only a weak cortical localization remained [6]. Overexpression of full-length coronin 3 on the other hand increased the number of cellular protrusions [6,7].

To investigate the role of coronin 3 on F-actin dynamics and the cytoskeleton *in vivo* we stably over-expressed in HEK293 cells the full-length protein (Coro3NWDC) or individual domains fused to EGFP and also reduced the amount of coronin 3 by RNAi silencing. The endogenous coronin 3 protein is referred to as Coro3WT. Coro3NC

contains the N-terminus fused to the C-terminus and lacks the five (conventional) central WD40-repeats. In Coro3NGC five glycine residues are inserted between N- and C-terminus replacing the five central WD40-repeats (Fig. 3A). Coro3WD contains the five central WD40-repeats. Expression of all the GFP-tagged proteins was confirmed by western blotting using a monoclonal anti-GFP antibody as well as the coronin 3-specific mAb K6-444. Normalized to the total protein concentration, the amounts of the fusion proteins were approximately one third (Coro3ΔCC), the same (Coro3ΔNC), two-fold (Coro3NC, Coro3NGC, Coro3WD), and four-fold increased (Coro3NWDC) compared to the endogenous protein. The amount of the endogenous protein was not changed upon transfection of the EGFP fusion proteins (data not shown).

Fixed cells were analyzed for morphology, cortical localization of coronin 3, and co-localization of coronin 3 with F-actin. The Coro3NWDC distribution paralleled the one of the endogenous coronin 3 (Fig. 1A, first panel, inset; HEK293: data not shown, refer to [6]) and showed a complete overlap with cortical F-actin (Fig. 3B). In contrast to HaCat cells (Fig. 1A, first panel, inset) HEK293 cells show a more pronounced staining of the submembranous area associated with a higher number of cellular protrusions. Coro3ΔNC was present throughout the cell but was not found at the cell cortex and induced a spindle like morphology in the cells [6]. Presence at the cortex was detected for Coro3NWDC and to a lesser extent for Coro3NGC (Fig. 3B, Table 1). A limited presence at the cell cortex as well was detected for Coro3ΔCC [6]. Proteins lacking the N-terminus and/or the central WD40 repeat domain, or being composed only of the central WD40 repeat were additionally observed in the nucleus (data not shown). None of the HEK293 cell populations showed altered subcortical F-actin structures. EGFP alone was uniformly distributed throughout the entire cell.

Triton X-100 treatment and differential centrifugation of HEK293 cells stably expressing Coro3NWDC, Coro3NC, Coro3NGC, or the endogenous protein only was performed as described above. The coronin 3-specific peak signals of the western blots indicate a soluble pool of coronin 3 (Trition wash) and an F-actin associated pool (100,000 g pellet). Coro3NC like Coro3NGC exhibits an association with F-actin (100,000 g pellet), although a submembranous localization was not visible in the immunofluorescence images. F-actin binding of Coro3NC seems to be insufficient for a subcortical localization and indicates the importance of intramolecular interactions between N- and C-termini *in vivo* (data not shown).

Coronin 3 accumulation follows the F-actin assembly during formation of protrusions

To gain insight into the temporal events during formation of cell protrusions we co-expressed Coro3NWDC, Coro3NGC, Coro3NC and Coro3ΔCC with RFP-actin in HEK293 cells. The proteins were followed at high magnification in living cells using confocal time-lapse microscopy. In cells expressing Coro3NWDC, Coro3NGC, and Coro3NC protruding cellular processes irrespective of becoming pseudopodia or filopodia show first an enrichment of actin (Fig. 4, Table 1). Images of segments of individual cells at time points 0, 10, and 20 seconds are shown. Between 0 and 10 seconds a protrusion appears or an existing protrusion elongates. At the 10-second time point, the protrusions indicate the highest signal intensities for RFP-actin (white-blue; NWDC), while the staining of EGFP-coronin 3 indicates clearly lower signal intensities (red) in the protrusions but a high accumulation in the back of the protrusions. Protrusions at the 10-second time point as well present nearly only RFP-actin signals (NGC, NC), but no staining of EGFP-coronin 3. At the 20 seconds time point, an intense signal of EGFP-coronin 3 occurred and co-localized with RFP-actin. In most cases the coronin 3 signal persists until the formation of the protrusion stops

and then decreases in parallel to the signal of RFP-actin or with a delay of a few seconds. These time course experiments suggest a role for coronin 3 shortly after the initial actin accumulation and presumably F-actin formation. After the observed delay Coro3NWDC, Coro3NGC, and Coro3NC co-localize with F-actin in the newly formed protrusions. The observed delay was detected in cells with similar intensities of the GFP- and RFP-signals but as well in cells with a prominent intensity of one of the fluorescent proteins. Monitoring of an additional transmission image (data not shown) ensured that only protrusions were analyzed. In cells expressing Coro3ΔCC, the coronin 3 and actin signals appear simultaneously in protruding cellular processes and do not change their levels significantly (Fig. 4; a lammellipodium spreads out between the filopodia). Coro3ΔCC was reported to forms dimers instead of trimers, which were shown to be important for the submembranous localization of the protein [6]; and data not shown). At all time points, the protrusions showed the same high signal intensities for GFP-Coro3ΔCC and for RFP-actin. In none of the experiments using Coro3ΔCC we noticed a delay in accumulation compared to RFP-actin.

Coronin 3 affects wound healing

To evaluate the contribution of coronin 3 to cellular processes we investigated wound healing of confluent layers of HEK293 cells stably expressing coronin 3 proteins. Wound healing was monitored over ten hours (Fig. 5A,B). We noted a statistically significantly reduced velocity of wound closure in case of all coronin 3 polypeptides compared to WT cells, which exhibited the fastest wound closure with an average velocity of 23 µm/h. Comparing the control Coro3NWDC (20 µm/h) with the other coronin 3 constructs demonstrated that except for Coro3ΔCC (21 µm/h) all constructs led to statistically significantly slower wound closure velocities. Cells, which express Coro3NC and Coro3NGC, lacking the central WD40 repeats or carrying a glycine

loop instead, showed reduced velocities of 14 µm/h and 15 µm/h, respectively. The strongest impairment in wound healing was noted for Coro3ΔNC (11 µm/h) and Coro3WD (11 µm/h). The latter results indicate a significant role for the F-actin binding domains, as well as for the central WD40 repeats, which generally are thought to function as a protein-protein interaction platform.

To further support the involvement of coronin 3 in wound healing we performed wound-healing assays with NIH3T3 fibroblasts in which the level of coronin 3 was significantly decreased by RNAi silencing. 48 hours after two treatments with a mixture of four different siRNA duplexes, confluent layers of wild-type NIH3T3 cells and siRNA transfected NIH3T3 cells were scratched and monitored over ten hours. RNAi treated cells showed a significantly delayed wound closure with an averaged velocity of wound closure of 25 µm/h compared to untransfected wild-type cells (33 µm/h). Control cells treated only with luciferase specific siRNA or with transfection reagent showed no impairment. Immunofluorescence images of coronin 3 siRNA treated cells did not reveal any obvious change and behaved like wild type in the F-actin staining, although the coronin 3-specific signal intensity was reduced in virtually all cells. The reduction of the coronin 3 expression was calculated from western blotting to be approximately 90% (Fig. 5C).

Coronin 3 influences cell proliferation and cytokinesis

As the prototype of the coronin protein family, *Dictyostelium discoideum* coronin, has been described to be involved in cell locomotion and cytokinesis [33], we addressed the effects of coronin 3 on cell proliferation and cytokinesis. Wild-type HEK293 and the stably transfected cell populations which exhibited differences compared to Coro3NWDC in the wound healing assay were seeded in low concentrations and counted again after three days to calculate cell proliferation. Coro3NWDC, Coro3NC,

Coro3NGC, and wild-type cells showed only slight and non-significant differences in cell proliferation. Statistically significant inhibitory effects were detected for cells transfected with Coro3ΔNC and Coro3WD (Fig. 6A).

To ascertain that the reduced cell proliferation is not caused by defects in cytokinesis, we repeated the experiment and determined the number of multinucleated cells after three days of cultivation (Fig. 6B). Wild type HEK293 cells and Coro3NWDC transfected cells showed the lowest levels of multinucleated cells. In contrast, cells transfected with any of the coronin 3 domain constructs showed approximately five-fold increased levels of multinuclear cells. An evaluation of the number of cells harboring two, three, or four and more nuclei detected no further differences.

Coronin 3 controls the formation of cellular protrusions

One major aspect of cell migration is the formation of cellular protrusions. Therefore, the activity of single wild type HEK293 cells or of cells expressing coronin 3 domains was recorded over 30 minutes (Fig. 7A). Figure 6 is representative for several experiments. Wild type HEK293 cells could not be distinguished from the Coro3ΔCC, Coro3NC, and Coro3NGC populations with regard to the number of protrusions formed. Coro3NWDC cells exhibit a slightly increased number of protrusions which was also detected by immunofluorescence images of fixed cells. A markedly reduced number of lamellipodia as well as filopodia was detected in HEK293 cell populations expressing Coro3ΔNC and Coro3WD. They further showed the lowest frequencies of changes in the number of forming or retracting protrusions (2.5 an 1.0, respectively). Although HEK293 populations expressing Coro3NC do not exhibit a change in the number of protrusions, the frequency of their formation is altered (Fig. 7B). The presence of the glycine loop between the N- and C-terminus (Coro3NGC) ameliorates the defect.

Coronin 3 affects fluid phase pinocytosis, but not receptor mediated endocytosis

To investigate further possible roles of coronin 3 at the submembranous cytoskeleton, the uptake of material was recorded. Phagocytosis is restricted to specialized mammalian cells and was not investigated. Fluorescent transferrin uptake was used to quantify the receptor-mediated and clathrin-associated endocytosis. This process was found to be unchanged in all HEK293 cell populations compared to the wild type (data not shown). In contrast, pinocytosis of the fluid phase marker HRP was significantly affected (Fig. 8). Coro3ΔNC and Coro3WD caused a distinctly reduced pinocytotic activity, while Coro3NC and Coro3NGC exhibited an intermediate decrease of pinocytosis.

Coronin 3 in PC-12 neurons alters axonal growth and norepinephrine secretion

The expression pattern of coronin 3 in the grey matter of the developing brain favors the assumption, that coronin 3 plays an important role during neuronal differentiation and migration [7]. We studied effects of the EGFP coronin 3 fusion proteins on the neuronal cell line PC-12, a rat phaeochromocytoma derived cell line. Wild-type cells and cells transiently expressing the full-length coronin 3 (Coro3NWDC) generally showed neurite (axon) extensions in more than 50% of the cells in response to NGF (Fig. 9A). The ratio between the fractions of very long neurites (neurite >4 soma) and smaller neurites (neurite ≤3 soma) was similar between these two populations. In contrast, cells expressing the other coronin 3 constructs showed clearly decreased levels of neurite formation or decreased neurite length, indicating a dominant negative effect on neurite elongation. In this assay Coro3NC and Coro3NGC showed the most impairment.

PC-12 cells are able to produce norepinephrine (noradrenaline). In addition to the cellular uptake assays described above, the secretion of the transmitter norepinephrine was measured in the absence (undifferentiated cells) and presence (differentiated cells; light upwards diagonals) of neurite growth factor (Fig. 9B). Generally, the presence of NGF reduced the secretion of norepinephrine. Wild-type cells showed the highest secretion levels of norepinephrine. A statistically significant reduction of the secretion was only detected in Coro3ΔNC and Coro3WD expressing cells, whereas cells expressing Coro3NC and Coro3NGC behaved like the Coro3NWDC population. The proportions of the secretion between undifferentiated and differentiated PC-12 cells remained constant in each individual cell population.

Coronin 3 forms a complex with the Arp2/3-complex and with cofilin

Previous studies had reported an interaction between yeast coronin and mammalian coronin 2 and the Arp2/3 complex [20-22]. Here we tested a complex formation with coronin 3. HEK293 cells expressing Coro3NWDC were used for several independent co-immunoprecipitation assays employing a monoclonal GFP-antibody (Fig. 10). Prior to harvest, the cells were treated with latrunculin B to prevent unspecific co-precipitation of proteins bound to and tied together by F-actin. Precipitated proteins were analyzed by the coronin 3 specific antibody detecting the endogenous as well as the EGFP-fusion protein. As expected, the endogenous coronin 3 binds to and coprecipitates with EGFP-coronin 3, most likely in a heterotrimeric complex [6]. Using antibodies specifically recognizing cofilin and the p34 (arc35) subunit of the Arp2/3 complex, we detected these proteins in the immunoprecipitate. For control we used BiP/GRP78- and ß-actin-specific antibodies excluding unspecific binding of the cell lysate or actin to the Protein G sepharose beads.

Discussion

Structure, in vivo subcellular localization and dynamics of EGFP-coronin 3

To date, the exact interactions and roles of most coronin proteins are still enigmatic as the biochemical or biological properties of only few of them have been characterized in detail within different species (for review see [5]). We previously identified coronin 3 as an actin filament crosslinking and bundling protein *in vitro*. In extension to our previous work on the biochemical characterization of coronin 3 [6] and its expression and distribution pattern in the developing murine brain [7], we address here the biological functions of coronin 3 in mammalian cells. The results are summarized in table 1.

Until a crystal structure of a coronin 1 fragment became available recently [2], the short conventional coronin proteins [5] were thought to consist of a N-terminal domain (aa 1-71) with a coronin-specific signature (aa 1-11), a core region containing five predicted WD40-repeats (aa 72-299), and a C-terminal domain (aa 300-474) with a very C-terminal coiled coil motif (aa 444-474). Based on the X-ray structure of the coronin 1 fragment, coronin 3 may contain two additional WD40-repeats. They are located in the regions referred to as N-terminus (aa 1-71) comprising aa 12-71 and in the conserved part of the C-terminus (aa 300-404) comprising aa 300-347. Both additional WD40-repeats are atypical in sequence and in structure [2]. The structural attributes, stabilizing intramolecular interactions of domains, and functional implications can be assigned to coronin 3 (see Results section). Particularly, surface areas of coronin 1 that *in silico* interact with F-actin can as well be assigned to coronin 3. Respective N- and C-terminal domains of coronin 3 have been used in our previous *in vitro* studies and were shown to be essential for F-actin binding [6], bundling and crosslinking [7]. This implicates that these expression construct

although harbouring only one WD40-repeat still fold properly and form functionally active domains. Our data from CD spectroscopy and thermal denaturation assays provide further evidence for proper folding. Therefore, domains of coronin 3 as well as the full-length protein appear to be useful to study its functional roles.

We confirmed the binding of coronin 3 to F-actin *in vivo* in human skin keratinocytes (HaCat) and further were able to describe the dynamics of coronin 3 and actin during formation of cell protrusions *in vivo* in HEK293 cells expressing EGFP-coronin 3 and RFP-actin using confocal time-lapse microscopy. A delay in the signal intensity of coronin 3 relative to the enrichment of actin suggests that during the initial stages of extension of cellular protrusions actin accumulates prior to coronin 3 and coronin 3 is not required for this process, indicating a tight spatial and temporal control of the coronin 3–F-actin interaction. One can propose that this behaviour is regulated by the seven-bladed WD40-repeat domain, which in general is thought to serve as a stable platform for simultaneous protein-protein interactions [3,4], however, this specific delay as well can depend on the presence of the C-terminal coiled coil domain. The coiled coil domain was shown to be important for subcortical localization of coronin 3, but was not found to be involved in F-actin binding [6]. In contrast to the trimeric three-dimensional structure of full-length coronin 3, the Coro3ΔCC-dimer might bind to F-actin in a non-regulated manner. The fact that coronin 3 locally enriched after the initial formation of a cellular protrusion and the underlying formation actin filaments points to a function of coronin 3 in the stabilization/maintenance of the steady state of the local actin network or in the inhibition of the further extension of the cellular protrusion.

Coronin 3 is important for F-actin dependent cellular processes

In a next step we analyzed the role of coronin 3 in further F-actin dependent cellular processes. In wound-healing assays the lack as well as the exclusive presence of the five central WD40-repeats most strongly inhibited the wound closure. These effects of coronin 3 domains and the fact that coronin 3 localizes to the cellular cortex prompted us to further investigate our findings in more detail regarding cell proliferation, cytokinesis, cell activity, endocytosis, secretion, and axonal outgrowth. As the N-terminus of coronin 3 interacts with the C-terminus [6], we generated Coro3NGC. Five glycine residues allow the formation of an intramolecular loop and our results demonstrated that Coro3NGC maintains the biological activity of the full-length protein in distinct cellular processes compared to Coro3NC (subcellular localization, frequency of changes in the number of protrusions). In most of the functional assays however, Coro3NC and Coro3NGC did not show a substantial difference, although Coro3NC exhibits a weaker association with F-actin, which is not visible at the immunofluorescence level, but detectable by differential centrifugation. The receptor-mediated clathrin-dependent endocytosis of fluorescently labeled transferrin appeared to be independent of coronin 3 although actin is thought to play a transient role in the formation of the vesicle [34,35]. On the other hand, fluid-phase endocytosis (macropinocytosis), which also depends on actin [36], was affected as well as the secretion of norepinephrine (noradrenaline) from PC-12 cells. PC-12 cells belong to the chromaffin cells, in which the process of exocytosis has been studied intensively [37]. Two pools of secretory vesicles (release-ready and reserve pool) are found in these cells and are separated by a cortical actin network [38]. Moreover, an exchange of secretory granules between these pools is facilitated by actin [39].

Coronin 3 and protein interactions

To elucidate possible mechanisms by which coronin 3 and the coronin 3 domain constructs exert their cellular role, we performed co-immunoprecipitations. Yeast coronin directly associates with the Arp2/3 complex, most likely via the Arc35 subunit, and exhibits an inhibitory function on the actin nucleation activity of the Arp2/3 complex [20,21]. The Arc35 binding motif is located in the coiled coil region of yeast coronin. Consistent with this observation C-terminally truncated murine coronin 1 did not bind to the Arp2/3 complex [2]. Likewise, mammalian coronin 2 was shown to bind to the p34 subunit of the Arp2/3 complex [22,40,41]. An inhibitory function of coronin 3 on the Arp2/3 complex would provide an explanation for some of our functional results. Our co-immunoprecipitation results support such a mechanism.

The central region of the growth cone contains a F-actin meshwork as well as F-actin bundles playing a central role in motility [40,41]. ADF/cofilins emerge as the key regulators of the axonal growth cone dynamics. Their severing activity is regulated by LIM kinases, slingshot phosphatases, and their upstream effectors [42]. Moreover, cofilin can act synergistically with the Arp2/3 complex to amplify local actin polymerization [43,44] in lamellipods. The outgrowth of neurites (axons) from PC-12 cells was strongly inhibited by Coro3NC and Coro3NGC. Coronin 3 could as well play a regulatory role in this different F-actin turnover process. It is noteworthy that yeast coronin interacts and synergizes with cofilin and accelerates the actin turnover via its WD40-repeat domain [45]. Mammalian coronin 4 was shown to bind to slingshot 1-L possibly by indirectly regulating the activity of cofilin [46].

From our data we conclude that coronin 3 acts in a complex manner on the formation and maintenance of actin-filaments. Coronin 3 peptides containing only the WD40-repeats act in a dominant negative manner most likely by competing for binding partners of coronin 3. The activity of coronin 3 may be mediated by interactions with other actin-binding proteins. Co-immunoprecipitation of cofilin and p34 in complex

with coronin 3 provided such specific interactions that can influence coronin 3-dependent cellular activities. Moreover, coronin 3 harbors an intrinsic F-actin bundling and crosslinking activity *in vivo* and *in vitro.* Therefore, both ablation and overexpression of coronin 3 considerably influenced cellular activities and coronin 3 peptides harboring only the F-actin binding domains and the coiled coil domain seem to act without specific regulation by putative binding partners demonstrating an inhibitory function. The largely unexplored coronin protein family clearly deserves further investigations and may turn out as a major modulator of actin dynamics.

Acknowledgements

We thank Dr. S. Wöll for providing the RFP-actin plasmid. This work was supported by the DFG (NO 113/13-3) and Köln Fortune.

References

[1] H.K. Fong, J.B. Hurley, R.S. Hopkins, R. Miake-Lye, M.S. Johnson, R.F. Doolittle, M.I. Simon, Repetitive segmental structure of the transducin beta subunit: homology with the CDC4 gene and identification of related mRNAs, Proc Natl Acad Sci U S A 83 (1986) 2162-6.

[2] B.A. Appleton, P. Wu, C. Wiesmann, The crystal structure of murine coronin-1: A regulator of actin cytoskeletal dynamics in lymphocytes, Structure 14 (2006) 87-96.

[3] D. Li, R. Roberts, WD-repeat proteins: structure characteristics, biological function, and their involvement in human diseases, Cell Mol Life Sci 58 (2001) 2085-97.

[4] T.F. Smith, C. Gaitatzes, K. Saxena, E.J. Neer, The WD repeat: a common architecture for diverse functions, Trends Biochem Sci 24 (1999) 181-5.

[5] V. Rybakin, C.S. Clemen, Coronin proteins as multifunctional regulators of the cytoskeleton and membrane trafficking, Bioessays 27 (2005) 625-32.

[6] Z. Spoerl, M. Stumpf, A.A. Noegel, A. Hasse, Oligomerization, F-actin interaction, and membrane association of the ubiquitous mammalian coronin 3 are mediated by its carboxyl terminus, J Biol Chem 277 (2002) 48858-67.

[7] A. Hasse, A. Rosentreter, Z. Spoerl, M. Stumpf, A.A. Noegel, C.S. Clemen, Coronin 3 and its role in murine brain morphogenesis, Eur J Neurosci 21 (2005) 1155-68.

[8] J.D. Sutherland, W. Witke, Molecular genetic approaches to understanding the actin cytoskeleton, Curr Opin Cell Biol 11 (1999) 142-51.

[9] F. Cvrckova, F. Rivero, B. Bavlnka, Evolutionarily conserved modules in actin nucleation: lessons from Dictyostelium discoideum and plants. Review article, Protoplasma 224 (2004) 15-31.

[10] C. Di Ciano, Z. Nie, K. Szászi, A. Lewis, T. Uruno, X. Zhan, O.D. Rotstein, A. Mak, A.S. Kapus, Osmotic stress-induced remodeling of the cortical cytoskeleton, Am J Physiol Cell Physiol 283 (2002) C850–C865.

[11] P.A. Rubenstein, K.K. Wen, Lights, camera, actin, IUBMB Life 57 (2005) 683-7.

[12] I.R. Nabi, The polarization of the motile cell, J Cell Sci 112 (Pt 12) (1999) 1803-11.

[13] A. Ponti, A. Matov, M. Adams, S. Gupton, C.M. Waterman-Storer, G. Danuser, Periodic patterns of actin turnover in lamellipodia and lamellae of migrating epithelial cells analyzed by quantitative Fluorescent Speckle Microscopy, Biophys J 89 (2005) 3456-69.

[14] T.E. Stradal, G. Scita, Protein complexes regulating Arp2/3-mediated actin assembly, Curr Opin Cell Biol 18 (2006) 4-10.

[15] T.D. Pollard, C.C. Beltzner, Structure and function of the Arp2/3 complex, Curr Opin Struct Biol 12 (2002) 768-74.

[16] H. Gournier, E.D. Goley, H. Niederstrasser, T. Trinh, M.D. Welch, Reconstitution of human Arp2/3 complex reveals critical roles of individual subunits in complex structure and activity, Mol Cell 8 (2001) 1041-52.

[17] J.A. Cooper, M.A. Wear, A.M. Weaver, Arp2/3 complex: advances on the inner workings of a molecular machine, Cell 107 (2001) 703-5.

[18] G.A. Strasser, N.A. Rahim, K.E. VanderWaal, F.B. Gertler, L.M. Lanier, Arp2/3 is a negative regulator of growth cone translocation, Neuron 43 (2004) 81-94.

[19] G.M. Popowicz, M. Schleicher, A.A. Noegel, T.A. Holak, Filamins: promiscuous organizers of the cytoskeleton, Trends Biochem Sci 31 (2006) 411-9.

[20] C.L. Humphries, H.I. Balcer, J.L. D'Agostino, B. Winsor, D.G. Drubin, G. Barnes, B.J. Andrews, B.L. Goode, Direct regulation of Arp2/3 complex activity and function by the actin binding protein coronin, J Cell Biol 159 (2002) 993-1004.

[21] A.A. Rodal, O. Sokolova, D.B. Robins, K.M. Daugherty, S. Hippenmeyer, H. Riezman, N. Grigorieff, B.L. Goode, Conformational changes in the Arp2/3 complex leading to actin nucleation, Nat Struct Mol Biol 12 (2005) 26-31.

[22] L. Cai, N. Holoweckyj, M.D. Schaller, J.E. Bear, Phosphorylation of coronin 1B by protein kinase C regulates interaction with Arp2/3 and cell motility, J Biol Chem 280 (2005) 31913-23.

[23] R.A. Kammerer, D. Kostrewa, P. Progias, S. Honnappa, D. Avila, A. Lustig, F.K. Winkler, J. Pieters, M.O. Steinmetz, A conserved trimerization motif controls the topology of short coiled coils, PNAS 102 (2005) 13891-6.

[24] T. Oku, S. Itoh, M. Okano, A. Suzuki, K. Suzuki, S. Nakajin, T. Tsuji, W.M. Nauseef, S. Toyoshima, Two regions responsible for the actin binding of p57, a mammalian coronin family actin-binding protein, Biol Pharm Bull 26 (2003) 409-16.

[25] N.-J. Hu, M. Currid, M. Daley, A. Hofmann, Two new software applications for automated processing of circular dichroism and fluorescence data., Appl Spectrosc 59 (2005) 68A.

[26] U.K. Laemmli, Cleavage of structural proteins during the assembly of the head of bacteriophage T4, Nature 227 (1970) 680-5.

[27] H. Towbin, T. Staehelin, J. Gordon, Electrophoretic transfer of proteins from polyacrylamide gels to nitrocellulose sheets: procedure and some applications, Proc Natl Acad Sci U S A 76 (1979) 4350-4.

[28] P. Boukamp, R.T. Petrussevska, D. Breitkreutz, J. Hornung, A. Markham, N.E. Fusenig, Normal keratinization in a spontaneously immortalized aneuploid human keratinocyte cell line, J Cell Biol 106 (1988) 761-71.

[29] C.S. Clemen, A. Hofmann, C. Zamparelli, A.A. Noegel, Expression and localisation of annexin VII (synexin) isoforms in differentiating myoblasts, J Muscle Res Cell Motil 20 (1999) 669-79.

[30] M.S. Springer, H.M. Blau, High-efficiency retroviral infection of primary myoblasts., Somat Cell Mol Genet 23 (1997) 203-209.

[31] A.A. Noegel, R. Blau-Wasser, H. Sultana, R. Muller, L. Israel, M. Schleicher, H. Patel, C.J. Weijer, The cyclase-associated protein CAP as regulator of cell polarity and cAMP signaling in Dictyostelium, Mol Biol Cell 15 (2004) 934-45.

[32] D.A. Ammar, P.N. Nguyen, J.G. Forte, Functionally distinct pools of actin in secretory cells, Am J Physiol Cell Physiol 281 (2001) C407-17.

[33] E.L. de Hostos, The coronin family of actin-associated proteins, Trends Cell Biol 9 (1999) 345-50.

[34] L.M. Traub, Common principles in clathrin-mediated sorting at the Golgi and the plasma membrane, Biochim Biophys Acta 1744 (2005) 415-37.

[35] C.J. Merrifield, M.E. Feldman, L. Wan, W. Almers, Imaging actin and dynamin recruitment during invagination of single clathrin-coated pits, Nat Cell Biol 4 (2002) 691-8.

[36] J. Liu, J.I. Shapiro, Endocytosis and signal transduction: basic science update, Biol Res Nurs 5 (2003) 117-28.

[37] M.F. Bader, R.W. Holz, K. Kumakura, N. Vitale, Exocytosis: the chromaffin cell as a model system, Ann N Y Acad Sci 971 (2002) 178-83.

[38] J. Trifaro, S.D. Rose, T. Lejen, A. Elzagallaai, Two pathways control chromaffin cell cortical F-actin dynamics during exocytosis, Biochimie 82 (2000) 339-52.

[39] T. Lang, I. Wacker, I. Wunderlich, A. Rohrbach, G. Giese, T. Soldati, W. Almers, Role of actin cortex in the subplasmalemmal transport of secretory granules in PC-12 cells, Biophys J 78 (2000) 2863-77.

[40] K. Kalil, E.W. Dent, Touch and go: guidance cues signal to the growth cone cytoskeleton, Curr Opin Neurobiol 15 (2005) 521-6.

[41] T.D. Pollard, G.G. Borisy, Cellular motility driven by assembly and disassembly of actin filaments, Cell 112 (2003) 453-65.

[42] R.A. Gungabissoon, J.R. Bamburg, Regulation of growth cone actin dynamics by ADF/cofilin, J Histochem Cytochem 51 (2003) 411-20.

[43] V. DesMarais, F. Macaluso, J. Condeelis, M. Bailly, Synergistic interaction between the Arp2/3 complex and cofilin drives stimulated lamellipod extension, J Cell Sci 117 (2004) 3499-510.

[44] V. DesMarais, M. Ghosh, R. Eddy, J. Condeelis, Cofilin takes the lead, J Cell Sci 118 (2005) 19-26.

[45] M. Gandhi, H.I. Balcer, B. Goode, Coronin functionally interacts with cofilin and Arp2/3 complex to regulate actin dynamics., Mol Biol Cell 16 (2005) Supplement: 456a (abstract 1681).

[46] T.W. Marshall, J.E. Bear, Coronin 2A expression regulates slingshot-1L activity., Mol Biol Cell 16 (2005) Supplement: 292a (abstract 1076).

[47] L.J. McGuffin, K. Bryson, D.T. Jones, The PSIPRED protein structure prediction server, Bioinformatics 16 (2000) 404-405.

Table 1

	WT	NWDC	ΔNC	NC	NGC	WD	ΔCC
cortical localization	**+**	**+**	**–**	**(+)**	**+**	**–**	**(+)**
focal enrichment	n.d.	**a<c**	n.d.	**a<c**	**a<c**	n.d.	**a=c**
wound healing	↔	↓	↓↓↓	↓↓	↓↓	↓↓↓	↓
cell proliferation	↔	↔	↓	↔	↔	↓	n.d.
# of nuclei	↔	↔	↑↑	↑↑	↑	↑↑	n.d.
protrusion #	↔	↑	↓↓	↔	↔	↓	↔
protrusion f	↔	↔	↓↓	↓	↔	↓↓	↔
transferrin uptake	↔	↔	↔	↔	↔	↔	n.d.
macropinocytosis	↔	↔	↓↓	↓	↓	↓↓	n.d.
secretion	↔	↓	↓↓	↓	↓	↓↓	n.d.
neurite outgrowth	↔	↔	↓	↓↓	↓↓	↓	n.d.
expression level	1	4	1	2	2	2	0.3

Summary of the effects of coronin 3 expression constructs (see Fig. 3) on various functional assays. **+** = yes, **–** = no, ↔ = wild type value; ↓ = decrease and ↑ = increase to different degrees compared to the wild type; **a<c** = actin accumulation prior to coronin, **a=c** = no difference in accumulation; n.d. = not determined. The expression level refers to the stably expressing HEK293 cell populations with compared to the WT.

Figure Legends

Fig. 1. Coronin 3 shows an F-actin dependent distribution in HaCaT cells. A, HaCaT cells treated with or without latrunculin B were either first fixed with 4% paraformaldehyde and then permeabilized with 0.2% Triton X-100 or first permeabilized and then fixed. Coronin 3 was detected using mAb K6-444 and goat-anti mouse-Cy3 as secondary antibody, F-actin was visualized using FITC-phalloidin. Inset first panel, a GFP-coronin 3 expressing HaCat cell as a control, color-coded in red. B, correspondingly, cells were incubated with or without latrunculin B and washed with Triton X-100 prior to additional washes with PBS and separation by differential centrifugation. Samples of the Triton X-100 washes and the centrifugation steps were analyzed by SDS-PAGE followed by western blotting using antibodies against coronin 3 and ß-actin. S, supernatant, P, pellet fractions.

Fig. 2. CD-spectroscopy and thermal denaturation of coronin 3 domains. A, far-UV CD spectra of coronin 3 (aa315-444, solid line) and coronin 3 (aa300-474, dashed line) in 20 mM NaCl, 5 mM HEPES, pH 7.5. Secondary structure prediction using these spectra yield between 25% and 30% ß-strand and about 60% random coil content, in agreement with the secondary structure prediction using PSIPRED [47]. Spectra were recorded at 20°C on a JASCO J-810 spectropolarimeter. Baseline correction, conversion into mean residue ellipticity and spectrum smoothing was carried out with ACDP [25]. B, thermal denaturation of coronin 3 (aa315-444, closed circles, solid line; T1/2=42°C) and coronin 3 (aa300-474, open circles, dashed line; T1/2=47°C). Both fragments show a standard two-state unfolding behaviour with the longer fragment possessing a higher transition temperature. The degree of unfolding was determined from constant monitoring of the CD signal at 222 nm. The sample

was heated from 20°C to 80°C at a rate of 1 K/min. Curve fitting was performed with SigmaPlot.

Fig. 3. Localization of full-length and truncated EGFP-coronin 3 fusion proteins in HEK293 cells. A, scheme of EGFP-constructs used. In addition, a scheme of coronin 3 is shown with the domains indicated as assigned from the coronin 1 crystal structure. B, HEK293 cells stably expressing EGFP-tagged domains of coronin 3 (upper panel) were fixed in 4% paraformaldehyde, permeabilized with 0.2% Triton X-100, and stained with TRITC-phalloidin (middle panel). Overlay, lower panel. Inset, the arrow indicates the presence of a faint cortical signal in these cells. C, corresponding to Fig. 1B, HEK293 cells were incubated with or without latrunculin B and washed with Triton X-100 prior to additional washes with PBS and separation by differential centrifugation. S, supernatant, P, pellet fractions.

Fig. 4. Emerging cellular protrusions indicate an accumulation of RFP-actin prior to GFP-coronin 3. Living HEK293 cells expressing GFP-Coro3NWDC, GFP-Coro3NGC, GFP-Coro3NC, or Coro3ΔCC and RFP-actin were monitored by confocal time-lapse microscopy. Every 10 seconds a 3-fold averaged image was taken. Images showing RFP-actin and GFP-coronin 3 alone are given, color-codes: red = low intensity, gold = high intensity, blue = maximum intensity. The overlay presents the merge of the original signals for RFP-actin (in red) and GFP-coronin 3 (in green). Each image represents a square of 7.5 x 7.5 µm.

Fig. 5. Coronin 3 knock down using siRNA as well as expression of EGFP-coronin 3 fusion proteins affect wound healing. A, the column on the left presents the wounds immediately after scratching a confluent HEK293 cell layer with a needle, the column

on the right presents the wounds after 10 hours. Cells expressing Coro3WT (endogenous coronin 3), Coro3NWDC, and Coro3NC are shown. Scale bar, 100 µm. B, Effect of coronin fusion proteins on wound healing. Error bars indicate the standard deviation from three independent experiments, each with three determinations of the width of the wound. p-values refer to the population expressing Coro3NWDC and were calculated by Student's t-test. C, representation of the wound healing behaviour of wt and siRNA treated NIH3T3 cells. Error bars indicate the standard deviation from three independent experiments, each with five determinations of the width of the wound. The western blot shows a ~90% reduction of the coronin 3 expression, immunofluorescence imaging as well indicate a decreased expression level of coronin 3, but no obvious change in the F-actin cytoskeleton. The p-value was calculated with single factor ANOVA. $p<0.05$ is significant.

Fig. 6. EGFP-coronin 3 fusion proteins affect cell proliferation and cytokinesis. A, proliferation rates of HEK293 cells expressing the indicated fusion proteins after three days of cultivation. The error bars represent the standard deviation of three independent experiments. p-values refer to the Coro3NWDC cell population and were calculated by Student´s t-test, $p<0.05$ is significant. B, bars indicate the number of cells having more than one nucleus per cell for different HEK293 cell populations. The values are from two independent experiments with approximately 185 cells analyzed per cell line.

Fig. 7. Coronin 3 fusion proteins alter the activity of HEK293 cells. The changes in the number of cellular protrusions including lamellipodia and filopodia followed over 30 minutes for the wt and cell populations expressing the coronin 3 polypeptides

indicated. A, the graph is representative for several independent experiments. B indicates the mean frequency of changes in the number of protrusions of each cell population over the time.

Fig. 8. Coronin 3 proteins influence fluid phase pinocytosis. HEK293 cells expressing coronin 3 fusion proteins were harvested and lysed after exposing them for 60 minutes to HRP-containing medium (2 mg/ml). The experiments were carried out three times in duplicate. The results were normalized to the total protein amount. p-values calculated by single factor ANOVA refer to the population of Coro3NWDC.

Fig. 9. Coronin 3 proteins alter neurite outgrowth and norepinephrine secretion in PC-12 cells. A, effect of coronin 3 proteins on the percentage of neurites of different length formed after four days of NGF treatment. Neurite (axon) lengths of PC-12 cells were defined as the distances from the tip of a neurite to the junction between neurite base and the cell body. The length of PC-12 neurites are given relative to the respective cell somata. B, effect of the coronin 3 fusion proteins on the norepinephrine (noradrenaline) secretion of NGF treated (light upward diagonal bars) and untreated (filled bars) PC-12 cells transiently transfected with the constructs indicated. The experiment was done twice. p-values refer to the Coro3NWDC cell population and were calculated by Student´s t-test, $p<0.05$ is significant.

Fig. 10. Endogenous coronin 3, p34-Arc, and cofilin co-immunoprecipitate with EGFP-Coronin 3. HEK293 cells expressing EGFP-Coro3NWDC were treated with latrunculin B and used for co-immunoprecipitation with an anti-GFP mAb. Samples were analyzed by immunoblotting using antibodies specifically recognizing coronin 3, p34-Arc, and cofilin (co-IP). For control the experiment was carried out with cell

lysate (beads only) or with anti-GFP mAb only, and the blot was probed with antibodies directed against BiP/GRP78 and ß-actin. Arrowhead, endogenous coronin 3; double-arrowhead, EGFP-coronin 3; arrow, p34 (arc35); asterisk, unspecific bands of the GFP-antibody solution. The signals for BiP/GRP78, coronin 3, and p34-Arc are from the same membrane probed serially; signals for ß-actin and cofilin are from parallel western blots.

Figure 1

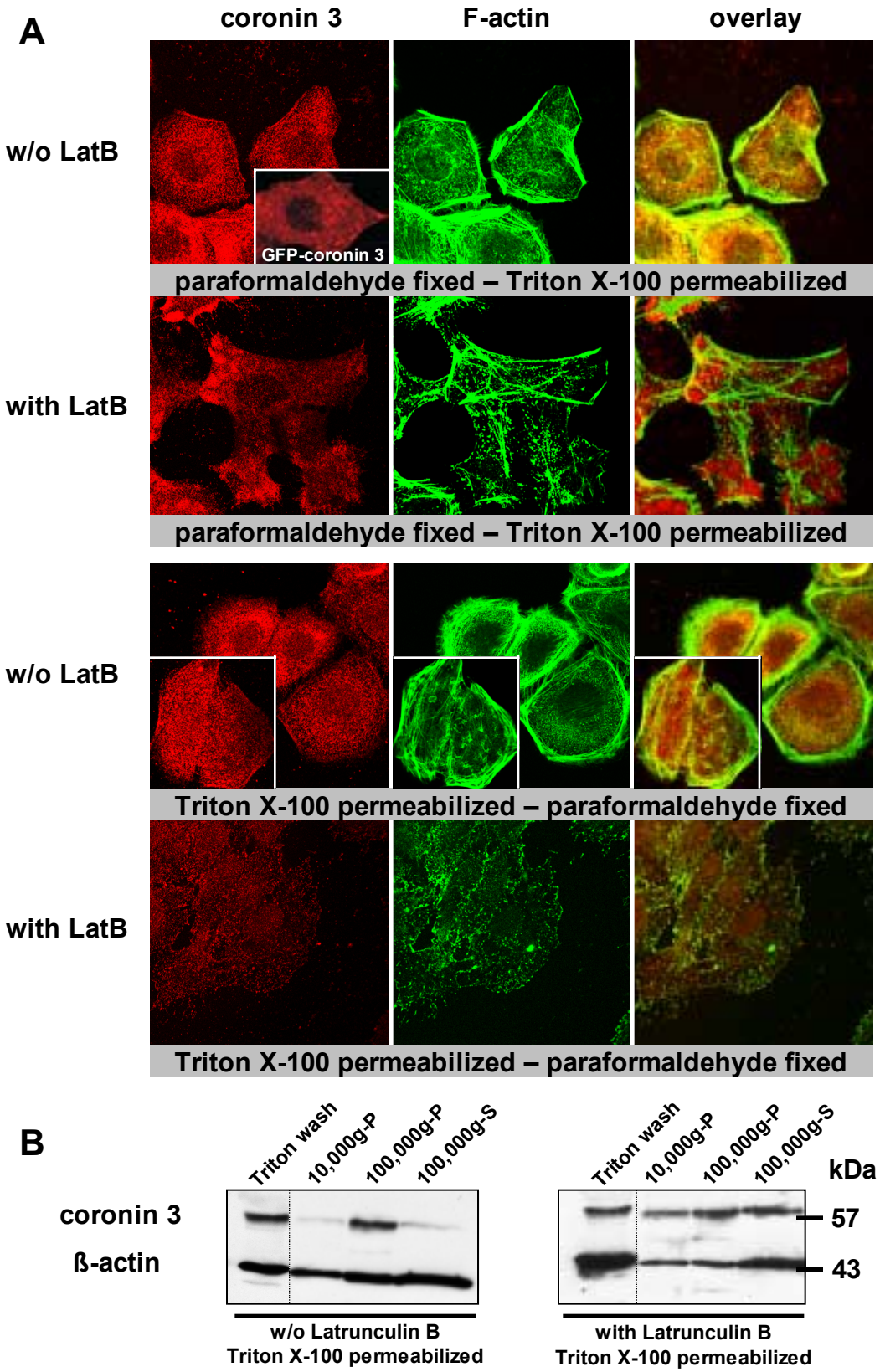

Figure 1

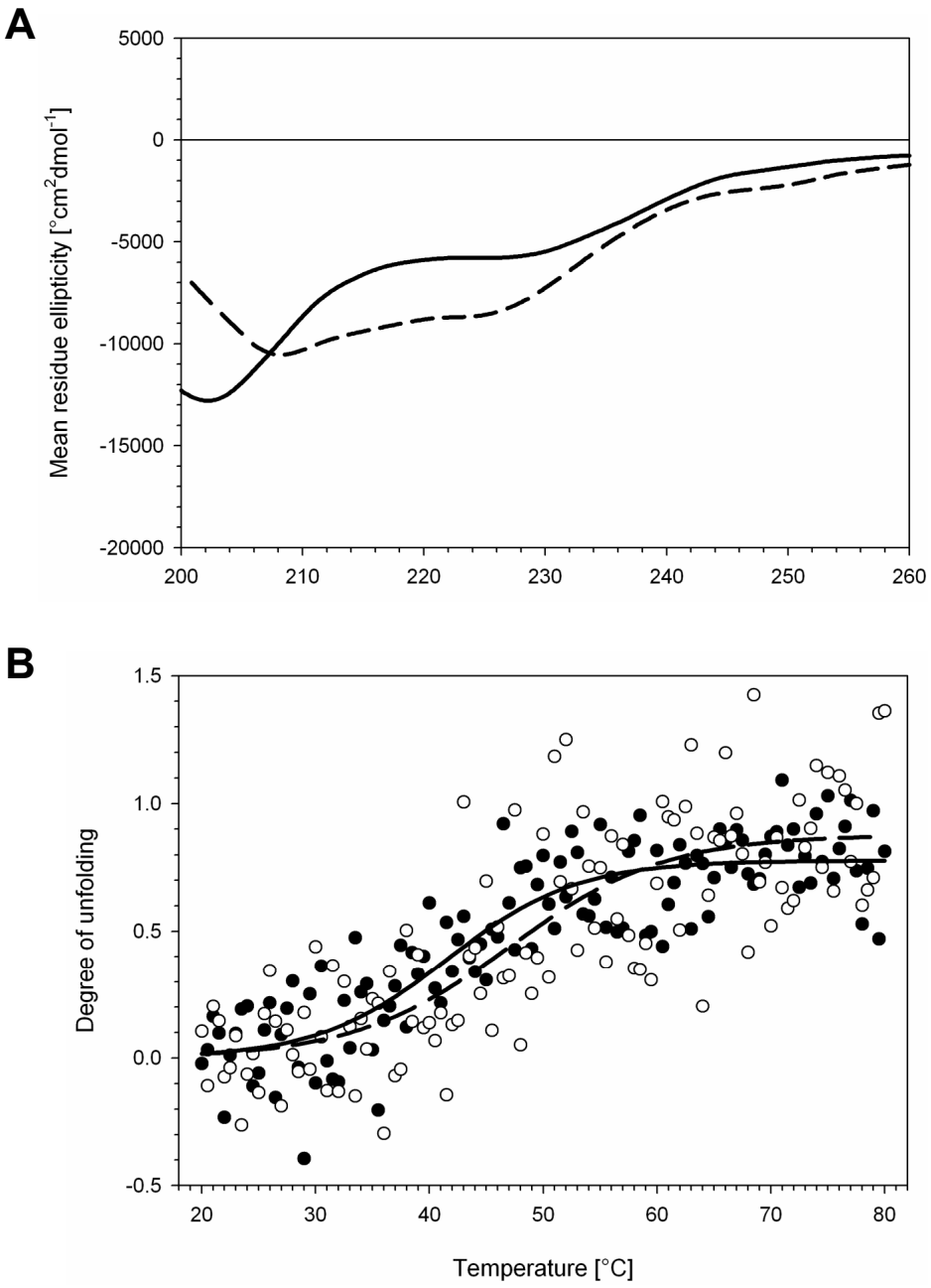
A
5000
0
-5000
-10000
-15000
-20000
Mean residue ellipticity [°cm²dmol⁻¹]
200
210
220
230
240
250
260
B
1.5
1.0
0.5
0.0
-0.5
Degree of unfolding
20
30
40
50
60
70
80
Temperature [°C]

Figure 2

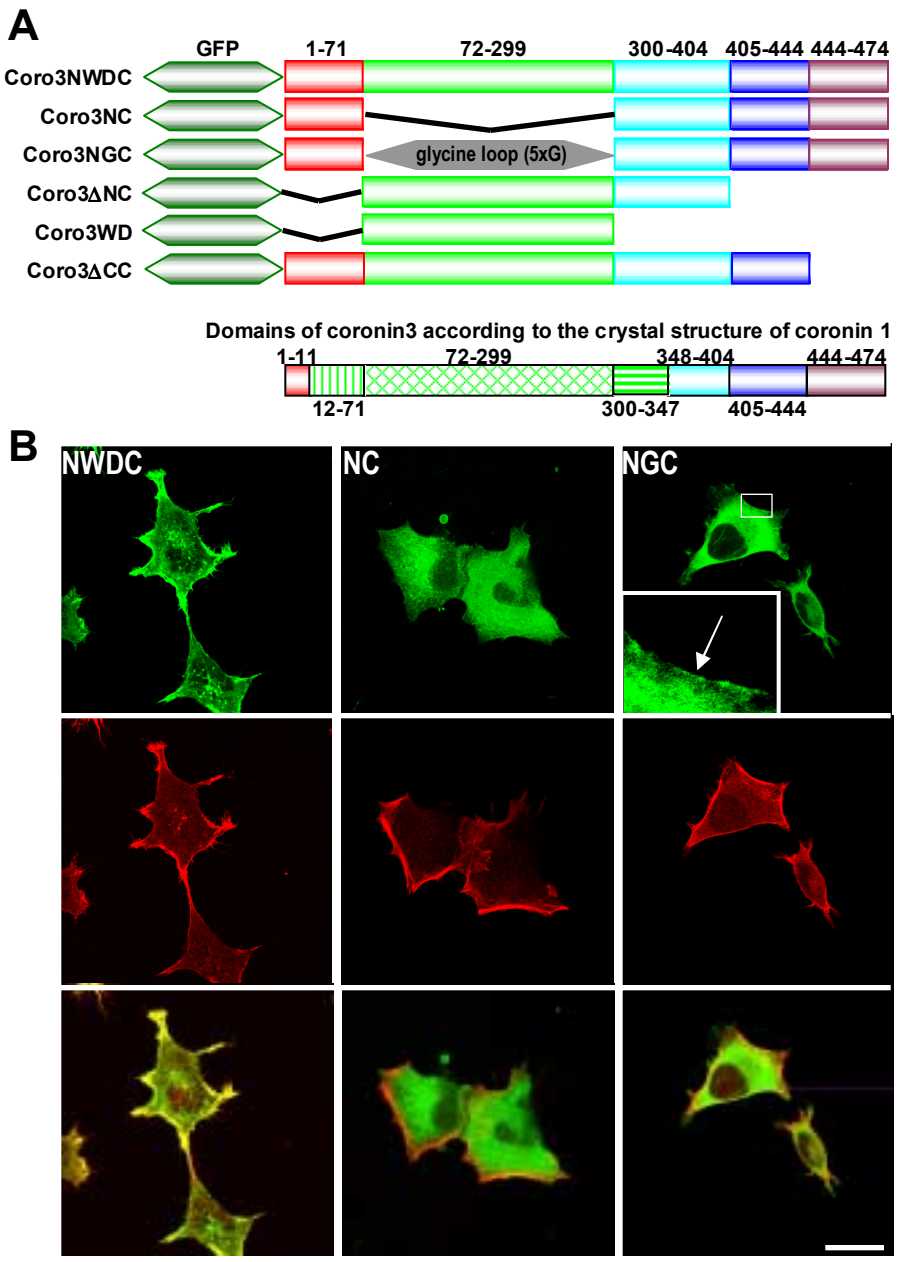
A
GFP
1-71
72-299
300-404
405-444
444-474
Coro3NWDC
Coro3NC
Coro3NGC
glycine loop (5xG)
Coro3ΔNC
Coro3WD
Coro3ΔCC
Domains of coronin3 according to the crystal structure of coronin 1
1-11
72-299
348-404
444-474
12-71
300-347
405-444
B
NWDC
NC
NGC

Figure 3

Figure 4

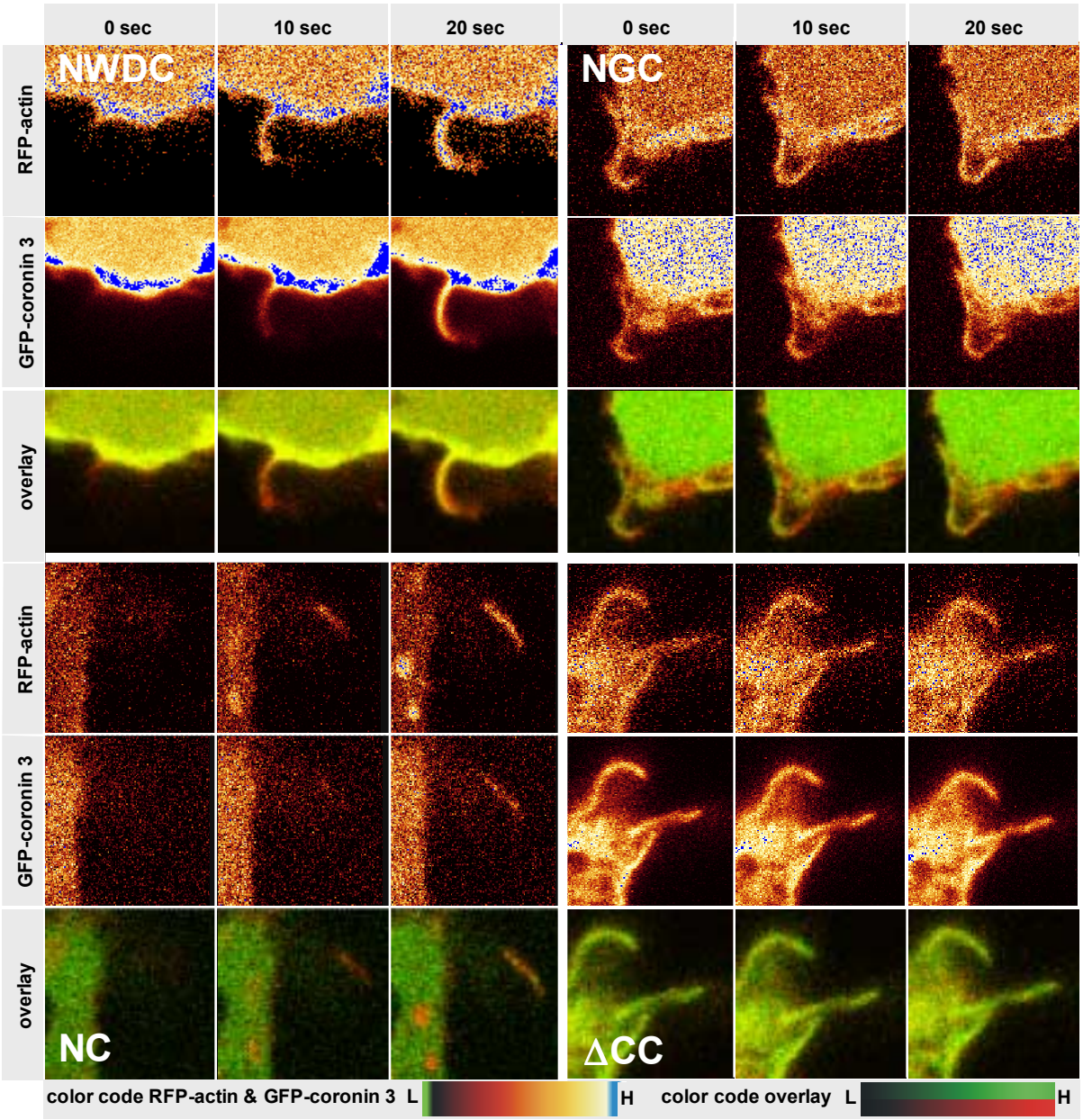

Figure 4

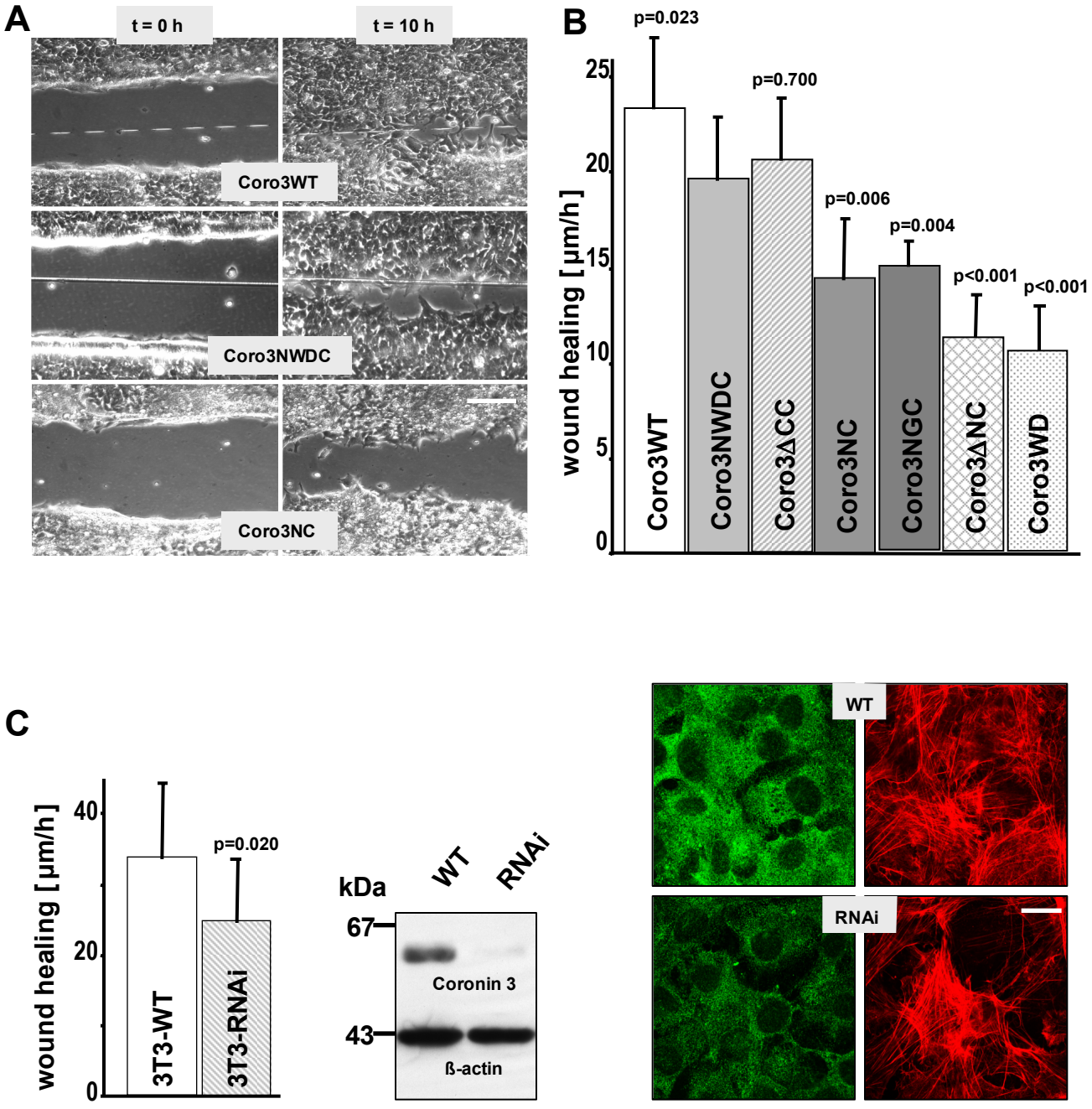
A
t = 0 h
t = 10 h
Coro3WT
Coro3NWDC
Coro3NC
B
wound healing [µm/h]
p=0.023
p=0.700
p=0.006
p=0.004
p<0.001
p<0.001
Coro3WT
Coro3NWDC
Coro3ΔCC
Coro3NC
Coro3NGC
Coro3ΔNC
Coro3WD
C
wound healing [µm/h]
p=0.020
3T3-WT
3T3-RNAi
kDa
WT
RNAi
67
43
Coronin 3
ß-actin
WT
RNAi

Figure 5

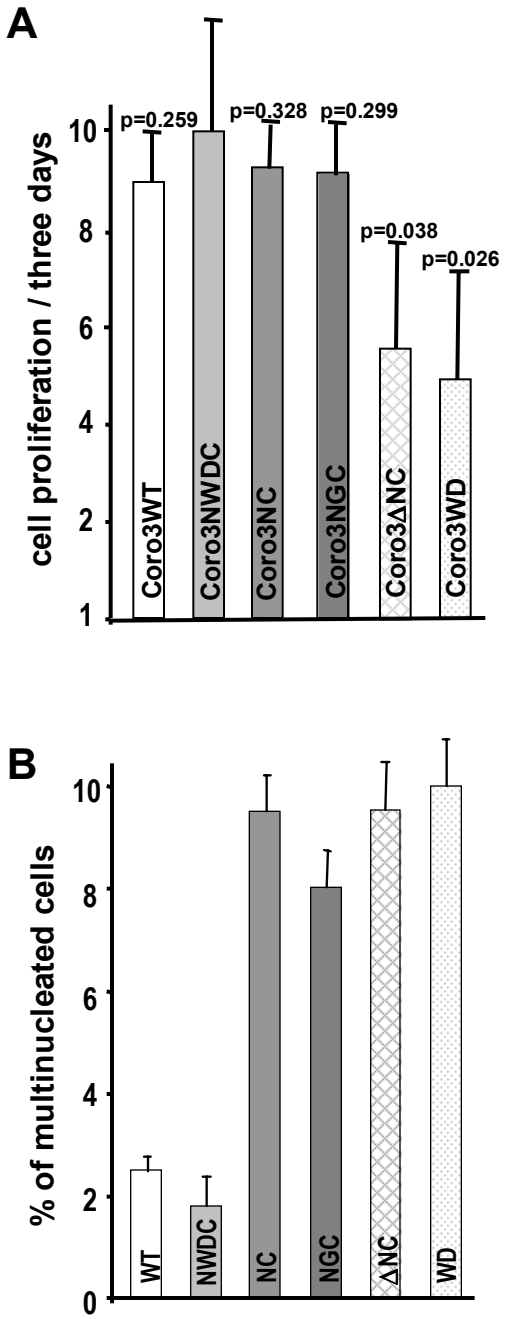
A
cell proliferation / three days
10
8
6
4
2
1
p=0.259
p=0.328
p=0.299
p=0.038
p=0.026
Coro3WT
Coro3NWDC
Coro3NC
Coro3NGC
Coro3ΔNC
Coro3WD
B
% of multinucleated cells
10
8
6
4
2
0
WT
NWDC
NC
NGC
ΔNC
WD

Figure 6

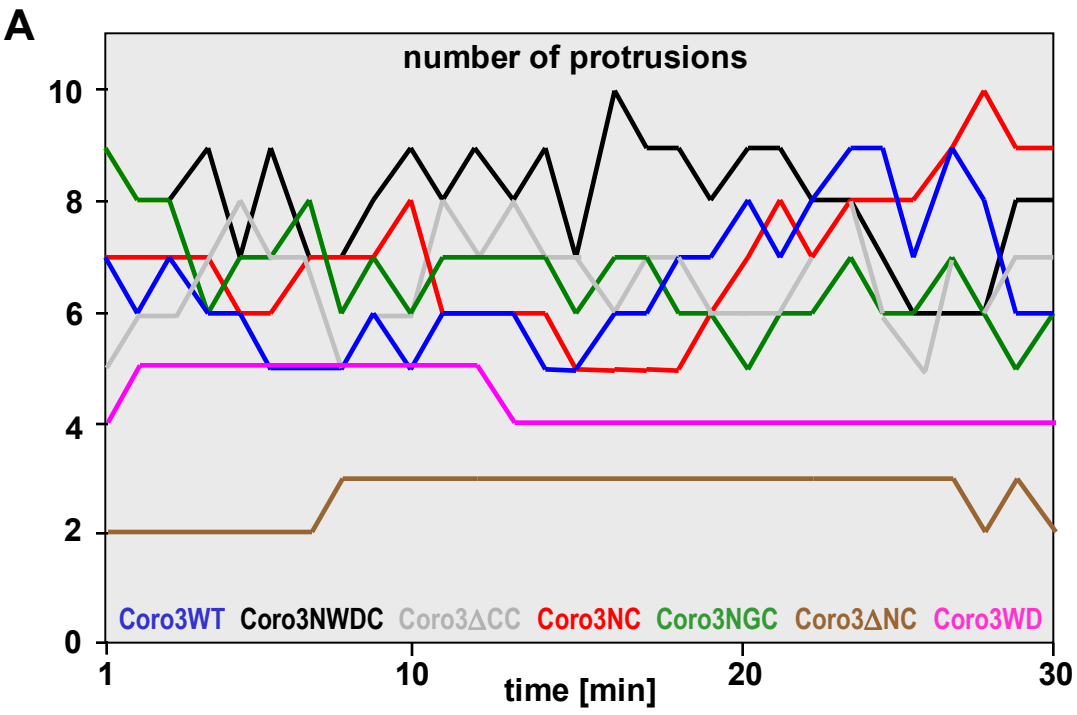

B

frequency of changes in the number of protrusions						
16.0	17.5	17.5	12.5	16.5	2.5	1.0
Coro3WT	Coro3NWDC	Coro3ΔCC	Coro3NC	Coro3NGC	Coro3ΔNC	Coro3WD

Figure 7

Figure 8

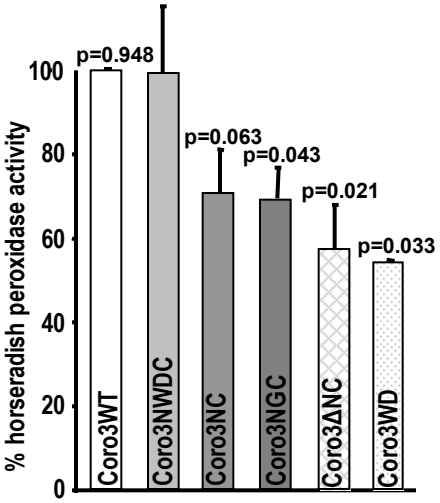

Figure 8

Figure 9

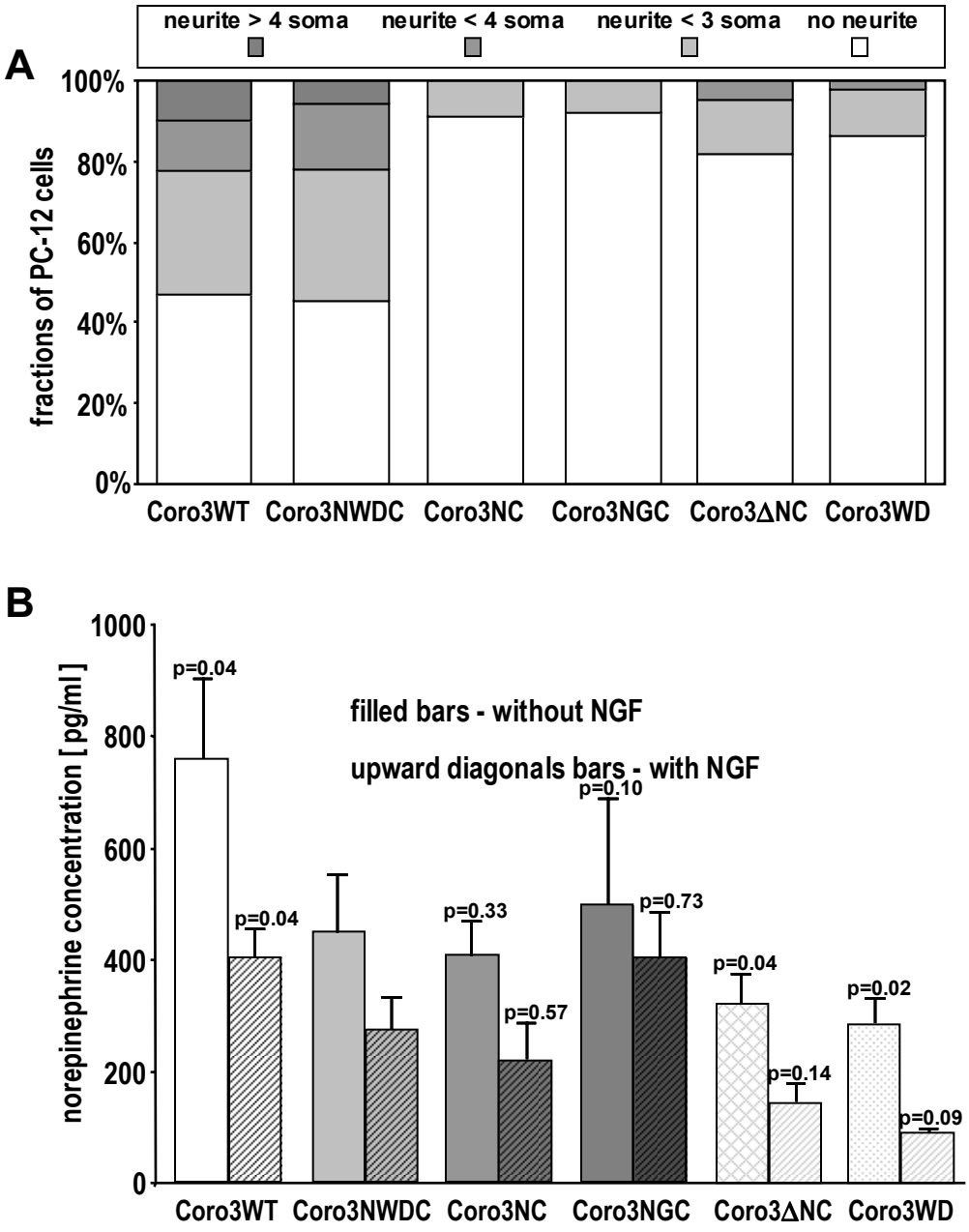

Figure 9

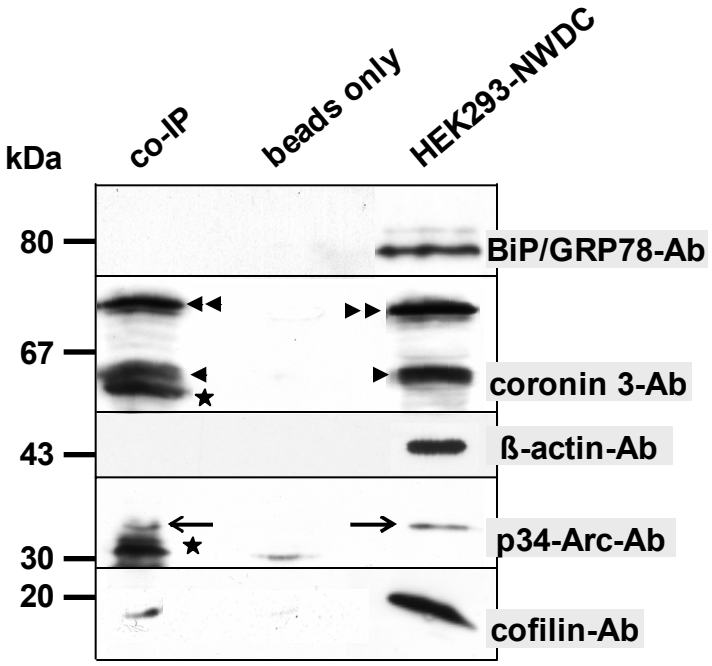
kDa
co-IP
beads only
HEK293-NWDC
80
67
43
30
20
BiP/GRP78-Ab
coronin 3-Ab
ß-actin-Ab
p34-Arc-Ab
cofilin-Ab

Figure 10